J Mater Sci (2009) 44:3488–3497
DOI 10.1007/s10853-009-3467-y

Tribological properties and high-speed drilling performance of Zr–C:H:$N_{x\%}$ coatings with different amounts of nitrogen addition

W. H. Kao

Received: 20 March 2008 / Accepted: 3 April 2009 / Published online: 20 April 2009

Abstract Zr–C:H:$N_{x\%}$ coatings with nitrogen additions ranging from 0 to 29 at.% are deposited on AISI M2 steel substrates and micro-drills using a closed field unbalanced magnetron (CFUBM) sputtering technique. The tribological properties of the coatings are tested against AISI 52100 steel balls under loads of 10 and 100 N, respectively, using an oscillating friction and wear tester. The drilling performance of the coated micro-drills is evaluated by performing high-speed through-hole drilling tests using printed circuit boards as a test material. The wear testing results reveal that the Zr–C:H:$N_{8\%}$ coating has excellent tribological properties, including a low wear depth, a low friction coefficient, and an extended lifetime. Meanwhile, the drilling tests reveal that the Zr–C:H:$N_{8\%}$ coating increases the tool life of the micro-drill by a factor of five compared to an uncoated micro-drill when used for the high-speed through-hole drilling of PCBs and yields a considerable improvement in the machining quality of the drilled hole.

Introduction

Diamond-like carbon (DLC) coatings are characterized by excellent mechanical and tribological properties, including low friction coefficients and a high wear resistance [1–6]. As a result, the literature contains many investigations into their basic physical, mechanical, and tribological properties, and their suitability for use in a range of practical applications [1, 7–13]. Broadly speaking, DLC coatings can be classified as either hydrogen-free (ta-C) or hydrogenated (a-C:H). In coatings of the former type, the carbon content is provided by a single graphite target during the deposition process, while in those of the latter type, the carbon content is obtained via the use of an appropriate reactive gas in the coating process. Researchers have demonstrated that the adhesion and tribological properties of a-C and a-C:H coatings can be enhanced via the addition of suitable amounts of metal dopants to produce so-called a-C:Me or Me-C:H coatings, respectively [14–20]. However, the past decade has witnessed a gradual trend away from the use of DLC coatings toward carbon nitride films on account of their favorable tribological [12, 21], electronic [22, 23], optical [24], and electron-chemical [25] properties. As a result, nitrogen-doped Me-C:H:N coatings have received comparatively little attention in the literature.

Accordingly, the current study performs a systematic investigation into the mechanical, adhesion, tribological properties, and high-speed drilling application of Zr–C:H:$N_{x\%}$ coatings with nitrogen additions ranging from 0 to 29 at.%. The coatings are deposited on AISI M2 steel substrates and micro-drills using a closed field unbalanced magnetron (CFUBM) sputtering process and the tribological properties of the coatings are then tested against AISI 52100 steel balls using a commercial oscillating friction and wear tester. The hardness of each coating is measured using a nanoindentation tester, while the adhesion properties are examined by performing scratch tests using a diamond stylus. Finally, the drilling performance of the coated micro-drills is evaluated by performing high-speed through-hole drilling tests using printed circuit boards (PCB) as a test material. Based on the experimental results and observations presented in this study, an assessment is made of the optimal Zr–C:H:$N_{x\%}$ coating for high-speed machining applications.

W. H. Kao (✉)
Institute of Mechatronoptic Systems, Chienkuo Technology University, Changhua, Taiwan
e-mail: n18851158@yahoo.com.tw

Experimental details

Coating deposition

Figure 1 presents a schematic illustration of the basic structure of the current Zr–C:H:$N_{x\%}$ coatings. The coatings were deposited on AISI M2 steel disks and micro-drills (MD020, Tera, Taiwan) using a CFUBM sputtering system (UDP-450, Teer Coating, UK) with a single zirconium target, three graphite targets, C_2H_2 and CH_4 reaction gas. Prior to the deposition process, the substrates were cleaned for 10 min in Ar plasma using a DC voltage of 350 V with a pulse frequency of 150 kHz. A Zr intermediate layer of thickness 0.1 μm was then deposited on the substrates using a chamber pressure of 3×10^{-3} Torr, a Zr target current of 0.7 A, and a bias voltage of −100 V. Subsequently, a a-C:Zr layer was deposited on the Zr film using a chamber pressure of 3×10^{-3} Torr, a Zr target current of 0.4 A, C target currents of 2 A, a frequency of 50 kHz and a bias voltage of −40 V. Finally, a-C:H:$N_{x\%}$ topcoats with nitrogen additions ranging from 0 to 29 at.% were deposited on the a-C:Zr layer by specifying an appropriate value of the N_2 reaction gas flow rate (see Table 1) while maintaining the remaining processing conditions as follows: a total chamber pressure of 3×10^{-3} Torr, a Zr target current of 0.4 A, C target currents of 2 A, C_2H_2 and CH_4 reaction gas flow rates of 3 sccm, a frequency of 50 kHz, a bias voltage of −40 V, and a table rotation speed of 3 rpm.

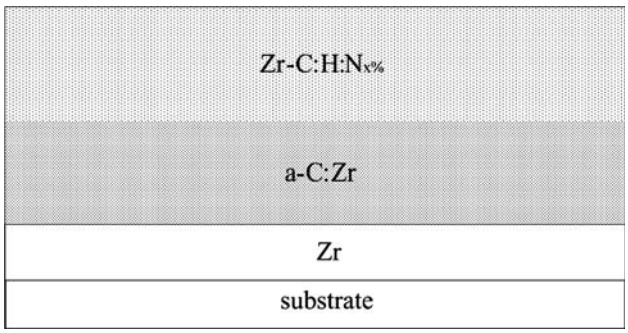

Fig. 1 Schematic illustration showing multi-layer structure of current Zr–C:H:$N_{x\%}$ coatings

Wear test

The basic tribological properties of the coatings were evaluated using the SRV (Schwingung Reibungund Verschleiss) oscillation friction and wear tester (Optimol, Germany) shown in Fig. 2. In the current wear experiments, the lower specimen was the coated AISI M2 disk with a hardness of 870 kgf/mm^2 and an average surface roughness of Ra = 0.008 μm, while the upper specimen was an AISI 52100 steel ball with a diameter of 10 mm and a hardness of 880 kgf/mm. Each wear test was performed for a total of 24 min using a constant stroke length of 1 mm, an oscillation frequency of 50 Hz, and a normal load of either 10 N or 100 N. In every case, the wear tests were performed under room temperature and atmospheric pressure conditions in an unlubricated condition. The relative humidity of the laboratory throughout the duration of the tests varied in the range 45–55%. Following each wear test, the maximum depth of the wear scar on the coated disk was measured using a surface profilometer (Kosake SE30H, Japan) with a precision of ±0.05 μm at a magnification of 2×10^4. Each coating was tested twice, with three separate depth measurements taken from each disk. The six maximum wear depth measurements obtained for each coating were then averaged to determine an overall wear depth value for the coating.

Hardness and adhesion tests

The hardness of each coating was measured using a nanoindentation tester (TriboScope, Hysitron Inc., Minneapolis, MN, USA) with a force at final contact of 1 mN. The adhesion properties of the coatings were examined by performing scratch tests, in which a diamond stylus with a diameter of 300 μm was driven across each coating under a continuously increasing loading rate of 1 N s^{-1}. The nominal maximum load was specified as 100 N and the critical load for each coating was defined as the value of

Table 1 Nitrogen flow rate, coating thickness, elemental composition, mechanical, and adhesion properties of current Zr–C:H:$N_{x\%}$ coatings

Coating	Nitrogen flow rate (sccm)	Coating thickness (μm)	Elemental composition (at.%)				Mechanical property Hardness (kgf/mm^2)	Adhesion property Critical load (N)
			C	Zr	N	H		
Zr–C:H:$N_{0\%}$	0	1.5	86	6.2	0	7.8	1463	63
Zr–C:H:$N_{8\%}$	1	1.8	85	2	8	5	1213	87
Zr–C:H:$N_{12\%}$	2	1.9	82	2	12	4	880	84
Zr–C:H:$N_{20\%}$	3	2.0	75	2	20.2	2.8	766	38
Zr–C:H:$N_{23\%}$	4	2.2	73	2	23.2	1.8	551	33
Zr–C:H:$N_{29\%}$	5	2.3	67	2	29.5	1.5	429	28

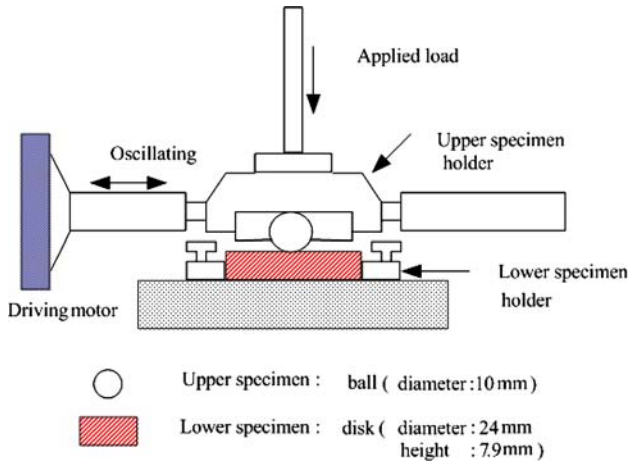

Fig. 2 Schematic illustration of SRV wear testing machine

the applied load at which the M2 disk first became visible at the base of the scratch track.

High-speed drilling tests

To investigate the suitability of the current Zr–C:H:$N_{x\%}$ coatings for industrial machining applications, the coated micro-drills were used in a series of high-speed through-hole drilling tests performed under dry conditions using PCB substrates. The drilling operation was performed using a commercial machining center (W1686-10, Schmol-Mashinen, Germany) with a drilling speed of 160,000 rpm (100.5 m/min) and a feed rate of 1.4 m/min (0.00875 mm/rev). The micro-drills were fabricated of AISI M2 steel with WC flute sections and had the following geometrical configuration: a diameter of 0.2 mm; an overall length of 38.1 mm; a fluted section length of 3.5 mm; a helix angle of 40°; and a point angle of 120°. The PCB used in the drilling tests measured 41 × 50 × 1.6 mm^3 and comprised eight copper layers embedded within FR-4; a fire-retardant resin epoxy reinforced with a fiberglass mat. Each drilling test was performed using two PCBs simply clamped together in the workpiece mounting system in the drilling machine.

The micro-drilling performance of each coated drill was evaluated by using an optical measurement system to measure the corner wear of the cutting edge following the drilling of 2,000 and 6,000 holes, respectively. Each coating was evaluated by performing two sets of drilling tests using a new micro-drill in each case. The wear value of each coating was then established by averaging the corresponding corner wear measurements obtained in the two tests.

Observation equipment

The coating surfaces, wear surfaces, and drilled holes were observed using optical microscopy (OM), scanning electron microscopy (SEM), and X-ray mapping (energy dispersive spectrometer, EDS) techniques. Meanwhile, the elemental composition of each coating was analyzed using glow discharge optical emission spectroscopy (GDOES). Finally, the cross-sectional thickness and wear morphology of each coating were determined using a scanning electron microscope (SEM).

Results

Composition, mechanical, and adhesion properties

Table 1 summarizes the nitrogen flow rates used to deposit each of the current coatings and indicates the corresponding coating thickness in every case. The table also shows the elemental composition of each coating together with the corresponding mechanical and adhesion strength properties. In general, the results indicate that the coating hardness reduces with an increasing nitrogen content. Thus, the Zr–C:H:$N_{0\%}$ coating has the highest hardness of 1463 Kgf/mm^2, while the Zr–C:H:$N_{29\%}$ coating has the lowest hardness of 429 Kgf/mm^2. Observing the results presented in Table 1 for the adhesion properties of the various coatings, it is clear that the critical load is highly sensitive to the level of nitrogen addition. The original coating has a relatively high critical load of 63 N. However, the addition of small amounts of nitrogen, i.e. 8 at.% or 12 at.%, increases the critical load to 87 and 84 N, respectively. In other words, nitrogen additions in the range 8–12 at.% yield a significant improvement in the adhesion strength of the Zr–C:H:$N_{x\%}$ coating. However, it is observed that for higher levels of nitrogen addition, i.e. 20–29 at.%, the critical load falls significantly to a value approximately one-half that of the original coating.

Tribological properties and lifetimes

In the wear tests performed in this study, the friction coefficients of the various point-contact wear pairs were continuously recorded under normal loads of 10 or 100 N. It was found that the friction coefficient curves associated with the lower normal load generally exhibited a low and stable value of the friction coefficient throughout the entire duration of the wear test. However, the friction coefficient curves recorded during the wear tests under a higher load comprised two distinct regimes, namely an initial region characterized by a low and stable value of the friction coefficient with an average value of μ_a and a second region characterized by a high, fluctuating value of the friction coefficient with an average value of μ_b. The lifetime (L) of each coating was defined as the duration of the first region in the friction coefficient curve, i.e., the elapsed time

Table 2 Wear testing results obtained for current Zr–C:H:$N_{x\%}$ coatings following sliding against AISI 52100 steel ball for 24 min under normal loads of 10 and 100 N, respectively

Coatings	Ball-on-disk point contact wear mode							
	Friction coefficient				Wear depth, D (μm)		Lifetime, L (s)	
	10 N		100 N		10 N	100 N	10 N	100 N
	μ_a	μ_b	μ_a	μ_b				
Zr–C:H:$N_{0\%}$	0.17	–	0.13	0.46	1.6	2.6	3384	1093
Zr–C:H:$N_{8\%}$	0.07	–	0.04	0.43	1.0	2.0	3418	1366
Zr–C:H:$N_{12\%}$	0.14	–	0.06	0.26	1.9	2.9	3126	1127
Zr–C:H:$N_{20\%}$	0.13	–	0.05	0.47	3.4	10.5	2675	646
Zr–C:H:$N_{23\%}$	0.16	–	0.08	0.52	3.6	19.5	2356	68
Zr–C:H:$N_{29\%}$	0.21	0.78	0.22	0.61	4.7	41.5	286	19
Uncoated	–	0.75	–	0.56	9.68	100.1	–	–

Note that μ_a denotes the average value of the low friction coefficient in the stable region of the friction coefficient curve, μ_b denotes the average value of the high friction coefficient in the fluctuating region of the friction coefficient curve, D denotes the depth of the wear scar on the coating following 24 min, and L denotes the lifetime of the coating, i.e. the duration from the start of testing until the time at which the friction coefficient suddenly increases and starts to fluctuate

between the start of the wear test and the moment at which the friction coefficient suddenly increased and became unstable. Table 2 summarizes the results obtained in the current experiments for the friction coefficients, the wear depths and the lifetimes of the current Zr–C:H:$N_{x\%}$ coatings under loadings of 10 and 100 N, respectively, following 24 min of wear testing. Figure 3 plots the wear depth and lifetime data presented in Table 2 for each of the Zr–C:H:$N_{x\%}$ coatings. The results show that the Zr–C:H:$N_{0\%}$, Zr–C:H:$N_{8\%}$, and Zr-C:H:$N_{12\%}$ coatings all have good tribological properties, i.e., a low wear depth and a long lifetime. From an inspection of the results presented in Table 2, it can be seen that the friction coefficients of these coatings vary between 0.07 and 0.17 under a low loading of 10 N and have lifetimes longer than 3126 s. At a higher loading of 100 N, the friction coefficients reduce (i.e., $\mu_a = 0.04$–0.13), and a long lifetime is still achieved, i.e., 1093–1366 s. Regarding the wear properties of the Zr–C:H:$N_{0\%}$, Zr–C:H:$N_{8\%}$, and Zr–C:H:$N_{12\%}$ coatings, Table 2 shows that the wear depths range from 1.0 to 1.9 μm under a loading of 10 N and from 2.0 to 2.9 μm under a loading of 100 N. Referring to Table 1, it is clear that the wear depth of the Zr–C:H:$N_{8\%}$ coating under a load of 10 N is less than the original coating thickness, while the wear depths of the Zr–C:H:$N_{0\%}$ and Zr–C:H:$N_{12\%}$ coatings are almost identical to the thickness of the original coating. Figure 3 shows that the coatings with a higher nitrogen content, i.e., Zr–C:H:$N_{20\%}$, Zr–C:H:$N_{23\%}$, and Zr–C:H:$N_{29\%}$, have an increased wear depth, i.e., between 3.4 and 4.7 μm under a loading of 10 N and between 10.5 and 41.5 μm under a loading of 100 N. For these three coatings, the wear depths are far greater than the original coating thickness, and hence the wear scars on the coated disk penetrate deep into the underlying substrate. Furthermore, it is apparent that higher levels of nitrogen addition result in a significant reduction in the coating lifetime, i.e., to <2675 s under a loading of 10 N and to <646 s under a loading of 100 N. The results presented in Table 2 and Fig. 3 clearly show that of the current coatings, the Zr–C:H:$N_{29\%}$ coating has the poorest tribological properties under both values of the normal load. For a normal load of 100 N, it is found that the wear depth (41.5 μm) is more than 20 times that of the Zr–C:H:$N_{8\%}$ coating (2.0 μm). Furthermore, the lifetime is just 19 s. In addition, it can be seen that the wear depths of the coatings with lower levels of nitrogen addition,

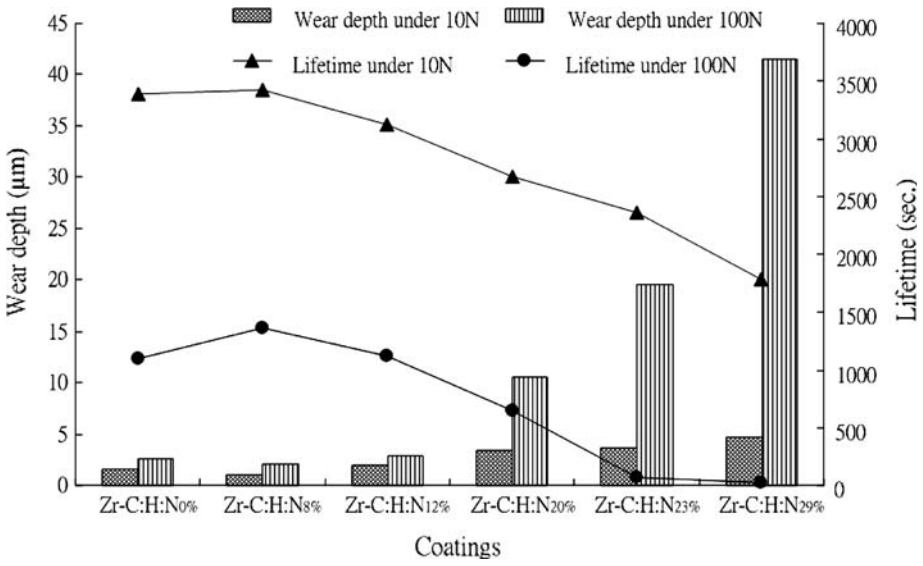

Fig. 3 Wear depth after 24 min testing, and lifetime of current Zr–C:H:$N_{x\%}$ coatings as evaluated in sliding against AISI 52100 steel ball under loadings of 10 and 100 N, respectively

i.e., Zr–C:H:$N_{0\%}$, Zr–C:H:$N_{8\%}$, and Zr–C:H:$N_{12\%}$, yield lower wear depths under a loading of 100 N than the Zr–C:H:$N_{20\%}$, Zr–C:H:$N_{23\%}$, and Zr–C:H:$N_{29\%}$ coatings under a lower loading of 10 N. Overall, the results show that of all the coatings considered in this study, the Zr–C:H:$N_{8\%}$ coating possesses the lowest wear depth: i.e., 1.0 and 2.0 μm under loadings of 10 and 100 N, respectively; the lowest friction coefficient: i.e., $\mu_a = 0.07$ and $\mu_a = 0.04$ under loadings of 10 and 100 N, respectively; and the longest lifetime: i.e., 3418 and 1366 s under loadings of 10 and 100 N, respectively.

High-speed drilling performance

To assess the suitability of the current coatings for industrial applications, a series of drilling tests were performed using coated micro-drills and PCB substrates. Figure 4 indicates the corner wear measurements of the various coated drills following the drilling of 2,000 and 6,000 holes, respectively. Note that the corner wear of an uncoated drill is also shown for comparison purposes. It is observed that the Zr–C:H:$N_{8\%}$ coating yields the lowest corner wear of all the drills. Significantly, the corner wear of this particular micro-drill after the drilling of 6,000 holes is lower than that of the uncoated micro-drill after the drilling of 2,000 holes. Conversely, the corner wear of the Zr–C:H:$N_{29\%}$-coated micro-drill is the highest of the current drills and is virtually identical to that of the uncoated drill, even at a lower number of drilled holes. The poor wear resistance of this particular coating is a result of its low hardness and adhesion strength properties (see Table 1). Defining the tool life as a corner wear of 34.4 μm (equivalent to the corner wear of an uncoated drill after drilling 2,000 holes), an experiment was performed to determine the maximum number of drilled holes attainable using a micro-drill coated with Zr–C:H:$N_{8\%}$ and an uncoated drill, respectively. The corresponding results are presented in Fig. 5 and indicate that the Zr–C:H:$N_{8\%}$-coated micro-drill is capable of drilling more than 10,000 holes before exceeding the maximum corner wear criterion of 34.4 μm. In other words, the Zr–C:H:$N_{8\%}$ coating increases the tool life of the micro-drill by a factor of five compared to an uncoated micro-drill.

Discussion

Tribological properties

During continuous wear testing under a load of 100 N, it was observed that all of the steel ball/coated disk wear pairs exhibited two principal wear behaviors. Figure 6

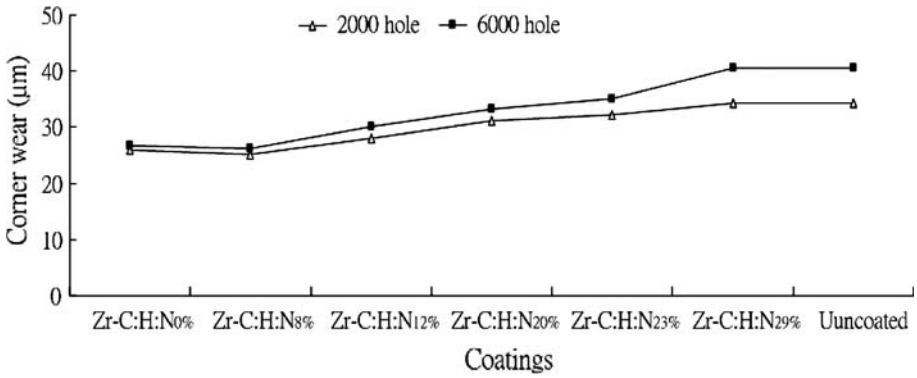

Fig. 4 Corner wear of current Zr–C:H:$N_{x\%}$ coatings following drilling of 2000 and 6000 holes, respectively

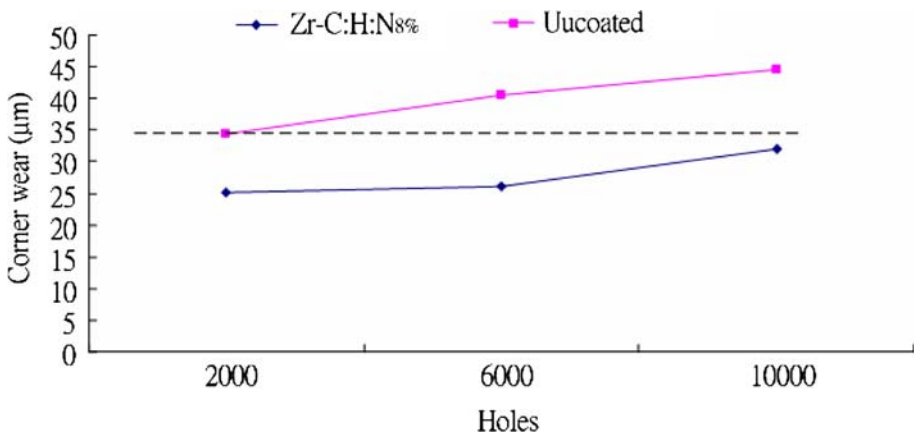

Fig. 5 Corner wear of Zr–C:H:$N_{8\%}$ coated micro-drill and uncoated drill following drilling of 2,000, 6,000 and 10,000 holes, respectively

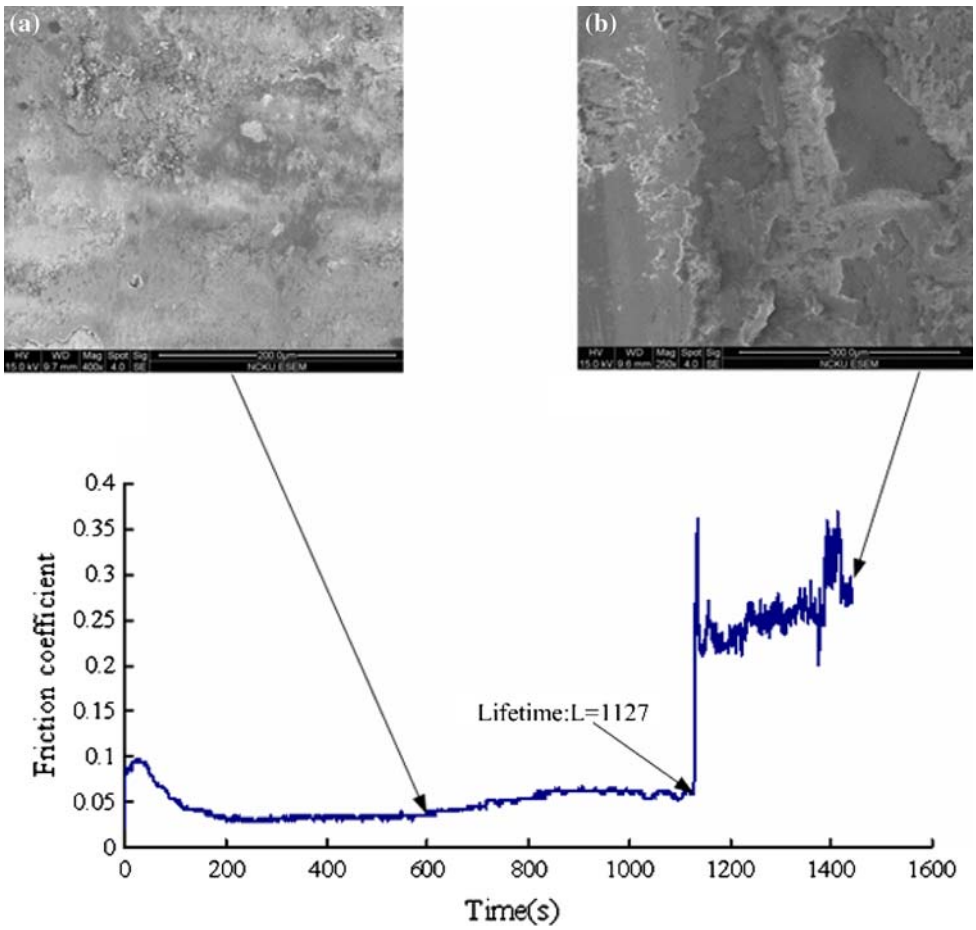

Fig. 6 SEM micrographs of wear scar on steel ball following sliding against Zr–C:H:$N_{12\%}$-coated disk for **a** 600 s and **b** 24 min under loading of 100 N

presents a typical friction coefficient curve corresponding to the steel ball/Zr–C:H:$N_{12\%}$-coated disk wear pair. As shown, the friction coefficient has a low, relatively stable value for the first 1127 s of the wear test, but then increases and becomes highly unstable as the wear test continues. The stable region of the friction coefficient curve indicates the presence of favorable tribological characteristics at the contact interface between the coated disk and the AISI 52100 steel ball, giving rise to a low friction coefficient and an improved wear resistance. Previous studies have reported that the formation of a thin transfer layer on the surface of the sliding counterbody reduces wear and friction effects in DLC/counterbody wear pairs [8, 26]. To examine the effect of the transfer layer on the tribological properties of the current steel ball/Zr–C:H:$N_{12\%}$-coated disk wear pair, the wear scars formed on the AISI 52100 steel ball counterbody were observed at various stages of the sliding test. The SEM micrographs presented in Fig. 6a and b show the surface morphologies of the steel ball wear scars after testing for 600 and 1440 s, respectively. The EDS analysis results obtained for the wear scar shown in Fig. 6a indicated an elemental composition of 38% carbon (atomic), 31% oxygen, 0.9% zirconium, and 30.1% Fe. The high carbon content of the wear scar indicates that a protective layer has been transferred from the Zr–C:H:$N_{12\%}$-coated disk to the AISI 52100 steel ball counterbody. The transfer layer improves the tribological properties of the wear pair by providing a solid lubricant effect, thereby protecting both the AISI 52100 steel ball and the Zr-C:H:$N_{12\%}$ coating from serious wear damage. For testing times greater than the coating lifetime (i.e., 1127 s in the current wear pair), Fig. 6 shows that the friction coefficient has a high fluctuating value, indicating a severe wear of both the AISI 52100 counterbody and the coated disk. An EDS analysis of the wear scar shown in the SEM micrograph presented in Fig. 6b reveals that the carbon content is reduced to 14.7 at.% while the oxygen content is increased to 50 at.%. In other words, the results demonstrate that the transfer layer formed on the AISI 52100 counterbody is completed eroded, resulting in a serious oxidative wear of the steel ball.

As shown in Table 2, under a lower loading of 10 N, all of the steel ball/coated disk wear pairs other than that comprising the disk with the Zr–C:H:$N_{29\%}$ coating exhibit a low friction coefficient throughout the entire duration of the wear test. Therefore, the coatings have a low wear depth and an extended life. The excellent tribological behavior of these coatings is attributed to the formation of a

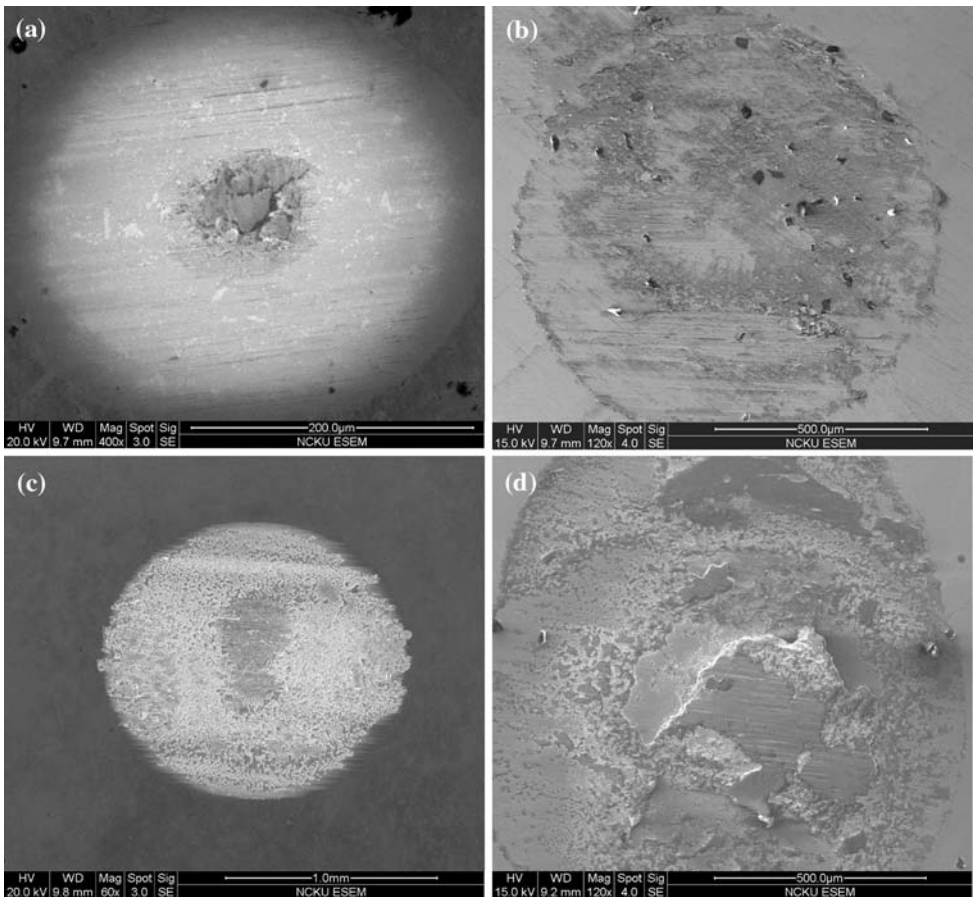

Fig. 7 Typical wear scars on steel ball/Zr–C:H:$N_{x\%}$-coated disk wear pairs following testing for 24 min under loading of 10 N: **a** Zr–C:H:$N_{8\%}$-coated disk and **b** steel ball; **c** Zr–C:H:$N_{29\%}$-coated disk, and **d** steel ball

transfer layer on the steel ball, as described in the paragraph above. Figure 7a and b presents SEM micrographs of the wear scars formed on the Zr–C:H:$N_{8\%}$ coating and the steel ball, respectively, following 24 min of wear testing. It is observed that the scar on the coating has a smooth appearance and has an accumulation of wear debris in its center. An EDS analysis of this wear debris shows that the carbon content is around 92.7 at.%. Thus, it is speculated that this debris represents an accumulation of the original coating in the central region of the wear scar as a result of the oscillatory nature of the wear process. Figure 7b clearly shows the formation of a transfer layer (indicated by the black regions and dots in the image) on the surface of the steel ball counterbody. The transfer layer is found to have a high carbon content of 68.7 at.% and therefore provides a solid lubricant effect which protects the Zr–C:H:$N_{8\%}$ coating from severe abrasive, oxidative, and adhesive damage, and therefore improves the tribological properties of the AISI 52100 steel ball/ Zr–C:H:$N_{8\%}$-coated disk wear pair. Of the current wear pairs, only the steel ball/Zr–C:H:$N_{29\%}$-coated disk exhibits a two-stage wear response under a load of 10 N. In performing wear testing using this particular coating, it was observed that a transfer layer was formed on the steel ball immediately that a reciprocating sliding motion was established between the steel ball and the coated disk. Consequently, the friction coefficient exhibited a stable and low characteristic (i.e., an average value of 0.21, see Table 2), and thus only a mild wear effect was observed at the contact surfaces of the wear pair. However, after 286 s, the value of the friction coefficient suddenly increased and became unstable, indicating the complete removal of the protective transfer layer on the steel ball and the coating on the disk, respectively. The erosion of the transfer layer eliminates the lubrication effect between the steel ball and the coated disk, and thus the friction coefficient increases significantly (to an average value of 0.78) prompting severe damage to the coating. Figure 7c and d presents SEM micrographs of the wear scars formed on the Zr–C:H:$N_{29\%}$ coating and the steel ball following 24 min of wear testing. It is apparent that both wear surfaces have a rough characteristic, indicating the occurrence of significant adhesive wear at the contact surfaces. The EDS analysis results reveal that the wear scar on the Zr–C:H:$N_{29\%}$ coating has a composition of 20.2% carbon (atomic), 0.8% Zr, 75.7% Fe, and 3.7% Cr, while that of the scar on the AISI 52100 steel ball has a composition of 31.9% carbon, 41.8% oxygen, and 26.3% Fe. The lower carbon content of the wear scar compared to that

observed in the wear scar shown in Fig. 7b confirms that the transfer layer is more readily removed during the sliding wear test when the coating has a high nitrogen content of 29 at.%. From Table 2, it can be seen that the wear depth of the Zr–C:H:$N_{29\%}$ coating is the highest of all the current coatings under a load of 10 N and has a value around 4.7 times higher than that of the Zr–C:H:$N_{8\%}$ coating. It can therefore be inferred that a high nitrogen content yields a poor tribological behavior in the current wear pairs, and results in a high friction coefficient, a high wear depth, and a reduced coating lifetime.

Drilling performance

Figures 8a–c presents SEM micrographs showing the worn cutting edges of an uncoated drill, a Zr–C:H:$N_{8\%}$-coated micro-drill and a Zr–C:H:$N_{29\%}$-coated micro-drill, respectively, following the drilling of 2,000 holes. In the drilling operation, the uncoated micro-drill adheres to the copper and epoxy resin within the PCB, and therefore tends to attract and retain chips as the drilling depth increases. This leads to an accumulation of chips on the cutting edge, causing the edge to become dull and rough (see Fig. 8a). However, the images presented in Fig. 8b and c reveal that the Zr–C:H:$N_{x\%}$ coatings improve the lubrication effect between the micro-drill and the workpiece, and therefore suppress the accumulation of chips on the cutting edge. The results presented in Table 1 show that the Zr–C:H:$N_{8\%}$ coating is characterized by a high hardness (1213 Kgf/mm^2) and a high adhesion strength (87 N). Furthermore, this coating has excellent tribological properties (as indicated in Table 2). Therefore, the SEM image presented in Fig. 8b shows the presence of a low corner wear following the drilling of 2,000 holes. Furthermore, it is apparent that a significant amount of coating (i.e., the black region in the image) remains on the micro-drill immediately below the cutting edge. Conversely, the Zr–C:H:$N_{29\%}$ coating has the lowest hardness and adhesion strength of the current coatings and exhibits poor tribological properties. As a result, the SEM micrograph shown in Fig. 8c shows evidence of significant corner wear and reveals the complete removal of the coating from both the cutting edge and the region of the micro-drill below the cutting edge.

Machining quality of drilled holes

Figure 9a–d shows the machining quality of the 2000th and 6000th holes drilled using an uncoated micro-drill (Figs. 9a and b) and a Zr–C:H:$N_{8\%}$-coated micro-drill (Fig. 9c and d), respectively. Figure 9a shows that the 2000th hole machined using the uncoated drill has a significant burred effect, while Fig. 9b shows that the 6000th drilled hole is severely distorted with blurring in evidence in and around the hole. By contrast, Fig. 9c and d shows that the use of a Zr–C:H:$N_{8\%}$ coating yields a significant improvement in the machining quality of both the 2000th hole and the 6000th hole. Significantly, it is noted that the quality of the 6000th hole is superior to that of the 2000th hole machined using the uncoated micro-drill. Therefore, it can be inferred that the Zr–C:H:$N_{8\%}$ coating not only increases the life of

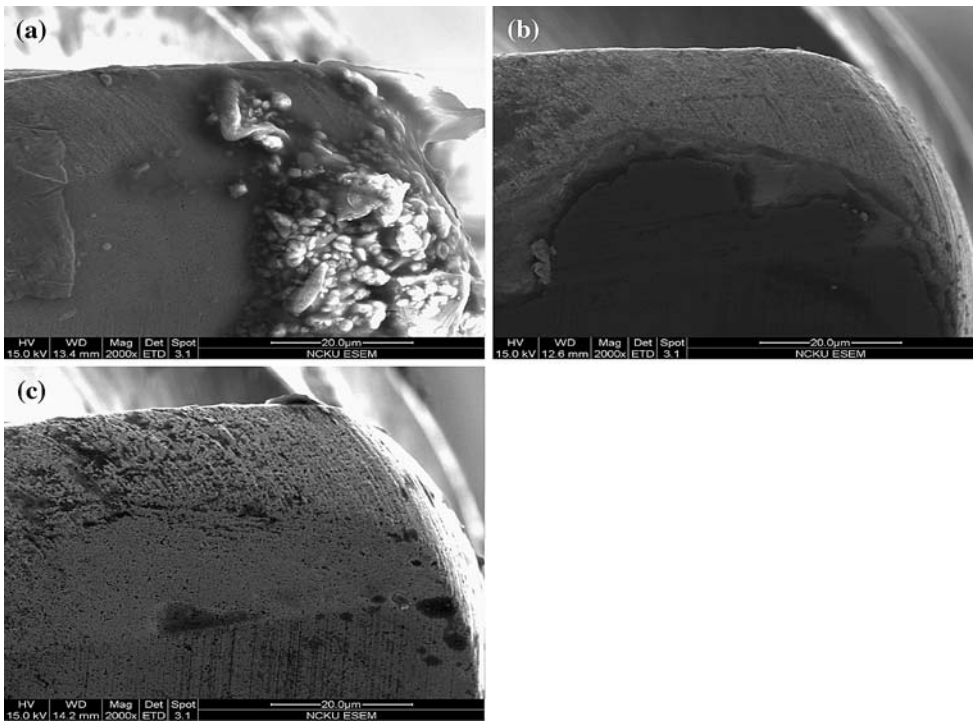

Fig. 8 Wear morphologies of various micro-drills following drilling of 2,000 holes: **a** uncoated drill, **b** Zr–C:H:$N_{8\%}$-coated drill, and **c** Zr–C:H:$N_{29\%}$-coated drill

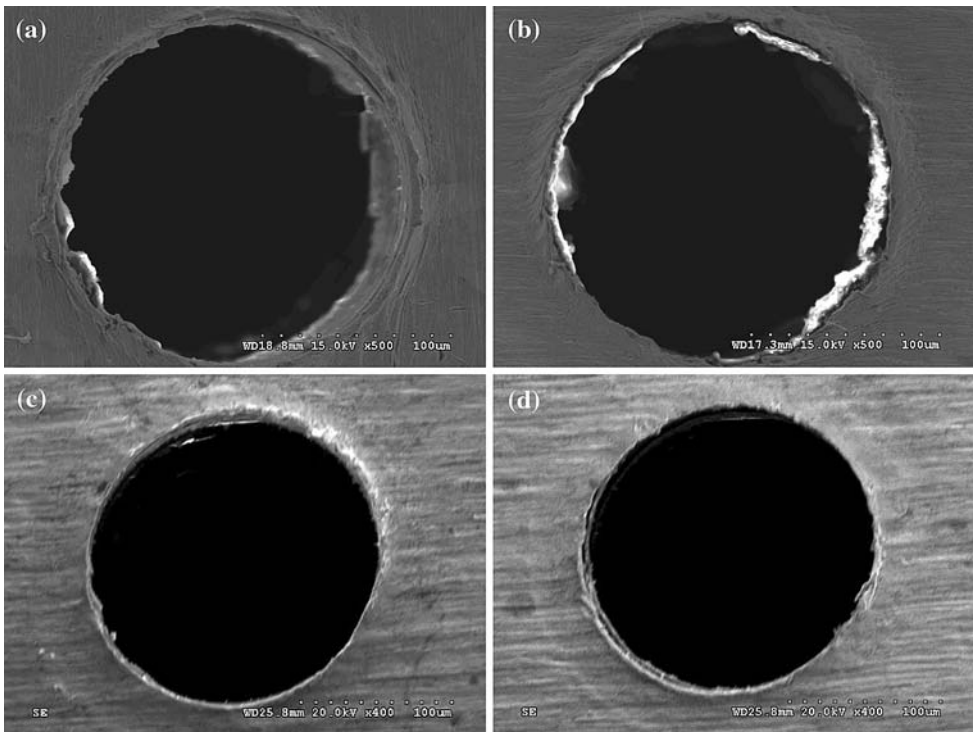

Fig. 9 Damage around drilled hole: **a** 2000th drilled hole and **b** 6000th drilled hole machined using uncoated micro-drill; **c** 2000th drilled hole, and **d** 6000th drilled hole using Zr–C:H:$N_{8\%}$ coated micro-drill

the micro-drill, but also improves the machining quality when applied to the high-speed through-hole drilling of PCBs under dry conditions.

Conclusions

The experimental results presented in this study support the following major conclusions:

1. The hardness of the Zr–C:H:$N_{x\%}$ coatings decreases as the nitrogen content increases. Thus, the Zr–C:H:$N_{0\%}$ coating has the highest hardness (1463 kgf/mm^2), while the Zr-C:H:$N_{29\%}$ coating has the lowest hardness (429 kgf/mm^2).
2. The adhesion strength of the Zr–C:H:$N_{x\%}$ coatings is highly sensitive to the level of nitrogen addition. The optimal coating adhesion strength is obtained with nitrogen additions of 8 at.% or 12 at.%, respectively.
3. The Zr–C:H:$N_{8\%}$ coating is found to be the optimal coating for sliding against an AISI 52100 steel ball due to the transfer of a solid lubricant layer from the coating to the surface of the steel ball. The transfer layer reduces the friction coefficient, improves the wear resistance properties of the wear pair, and extends the coating lifetime.
4. The Zr–C:H:$N_{8\%}$ coating increases the lifetime of the micro-drill by a factor of five times compared to an uncoated drill and yields a significant improvement in the quality of the drilled hole.

Acknowledgement The author would like to thank the National Science Council of the Republic of China for financially supporting this research project under Contract No. NSC 96-2212-E270-011.

References

1. Harris SJ, Weiner AM, Meng WJ (1997) Wear 211:208
2. Ronkainen H, Varjus S, Koskinen J, Holmberg K (2000) Wear 249:260
3. Zhang W, Tanaka A (2004) Tribol Int 37:975
4. Ohana T, Nakamura T, Suzuki M, Tanaka A, Koga Y (2004) Diamond Relat Mater 13:1500
5. Kao WH, Su YL, Yao SH, Luan JM (2005) Mater Sci Eng A 398: 233
6. Charitidis C, Logothetidis S (2005) Thin Solid Films 482:120
7. Deng J, Bran M (1995) Diamond Relat Mater 4:936
8. Liu Y, Erdenir A, Meletis EI (1996) Surf Coat Technol 82:48
9. Ronkainen H, Likoen J, Koskinen J, Varjus S (1996) Surf Coat Technol 79:87
10. Sheeja D, Tay BK, Krishnan SM, Nung LN (2003) Diamond Relat Mater 12:1389
11. Wei Z, Akihiro T (2004) Tribol Int 37:975
12. Yan X, Xu T, Chen G, Yang S, Liu H (2004) Appl Surf Sci 236: 328
13. Yuichi A, Naoto O (2004) Tribol Int 37:941
14. Narayan RJ (2005) Appl Surf Sci 245:420
15. Miyake S, Saito T, Yasuda Y, Okamoto Y, Kano M (2004) Tribol Int 37:751
16. Inkin VN, Kirpilenko GG, Dementjev AA, Maslakov KI (2000) Diamond Relat Mater 9:715
17. Yang S, Camino D, Jones AHS, Teer DG (2000) Surf Coat Technol 124:110
18. Wang DY, Chang CL, Ho WY (1999) Thin Solid Films 355–356: 246

19. Wei Q, Narayan RJ, Narayan J, Sankar J, Sharma AK (1998) Mater Sci Mater B 53:262
20. Dimigen H, Hübsch H, Memming R (1987) Appl Phys Lett 50: 1056
21. Scharf TW, Ott RD, Yang D, Barnard JA (1999) J Appl Phys 85: 3142
22. Allon M, Croitoru N (1997) Diamond Relat Mater 6:555
23. Guerino M, Massi M, Maciel HS, Otani C, Mansano RD (2003) Microelectr J 34:639
24. Klibanov L, Croitoru N, Seidman A, Scheffer L, Ben-Jacob E (1997) Diamond Relat Mater 6:1868
25. Liu LX, Liu E (2005) Surf Coat Technol 198:189
26. Liu H, Tanaka A, Kumagai T (1999) Thin Solid Films 352:145